# PROBABILISTIC NUMERICAL LIMIT ANALYSIS OF 2D AND 3D SLOPES CONSIDERING SPATIAL VARIABILITY OF SHEAR STRENGTH PARAMETERS

David Sebastian Calpa
Pontifical Catholic University of Rio de Janeiro, Rio de Janeiro, Brazil, sebastiancalpaj@gmail.com

Raquel Quadros Velloso
Pontifical Catholic University of Rio de Janeiro, Rio de Janeiro, Brazil, raquelvelloso@puc-rio.br

Euripedes Vargas Jr
Pontifical Catholic University of Rio de Janeiro, Rio de Janeiro, Brazil, eavargasjr@gmail.com

Fabricio Fernández
Universidad Católica del Norte, Antofagasta, Chile, fabricio.fernandez@ucn.cl

**ABSTRACT:** Numerical Limit Analysis (NLA), although little known and used, is a powerful technique to efficiently determine the stability conditions in slopes. In this paper, we extend the application of the NLA by including a probabilistic framework to capture the spatial variability of soil shear strength parameters. To achieve this, stationary, unconditional, multivariate, cross-correlated random fields were implemented on an existing, in-house developed computer code, employing both conventional and stepwise Covariance Decomposition Methods (CMD). In order to verify the implemented code in terms of efficiency and robustness, 2D and 3D problems were analyzed. The paper demonstrates that NLA is a robust alternative to standard methods such as the limit equilibrium and finite element method with the strength reduction technique. Emphasis is placed on the significance of incorporating autocorrelation and cross-correlation to realistically represent spatial variation in parameters and address uncertainties associated with soil shear strength.

KEYWORDS: Probabilistic Numerical Limit Analysis, Safety factor, Collapse factor, Probability of failure, Random Fields, Covariance Decomposition Method

## 1 INTRODUCTION

Slope engineering is perhaps the geotechnical subject most dominated by uncertainty. Geological anomalies, inherent spatial variability of soil properties, scarcity of representative data, changing environmental conditions, unexpected failure mechanisms, simplifications and approximations adopted in geotechnical models and human mistakes in design and construction, are all factors contributing to uncertainty (El-Ramly et al., 2002). In response to the inherent uncertainty surrounding the definition of soil shear strength parameters, conventional engineering practices frequently employ probabilistic analysis utilizing a Single Random Variable (SRV) approach, where one-point statistical parameters such as the mean and variance of shear strength parameters are specified and exhibit complete correlation at any point in the model. This approach suffers a significant drawback: it cannot account for the spatial structure and averaging of the soil properties, potentially resulting in inaccurate predictions of failure mechanisms and safety factors (Fs) (Ou-Yang et al., 2021). Over the past two decades, significant progress has been achieved in probabilistic analysis by integrating Random Fields (RFs) to address the spatial variability of soil parameters. Concerning shear strength parameters, certain studies have incorporated the undrained shear strength ($s_u$) (Griffiths & Fenton, 2000a, 2000b; Hicks & Samy, 2002; Jiang & Huang, 2018; Zhu et al., 2021) while others have integrated both cohesion ($c$) and friction angle ($\phi$) (Cho, 2007; Li et al., 2015; Tang et al., 2020; M. Y. Wang et al., 2020;

Z.-Z. Wang & Goh, 2021), as spatial random variables, within a probabilistic framework. The primary methods utilized in conjunction with RFs generation techniques, to evaluate the slope stability margin have traditionally been the Limit Equilibrium Method (LEM) and the finite element method (FEM). Despite its computational efficiency, LEM suffers from a significant drawback: the requirement to assume the shape and location of the slope failure surface. This limitation prevents the identified mechanism from naturally finding the most critical path through the soil (Griffiths & Fenton, 2004). Alternatively, the incorporation of FEM leads to a more rigorous probabilistic analysis. This method does not require a priori assumptions concerning the shape or location of the failure surface. However, it stills faces a significant limitation: the extensive computational efforts needed when working with multiple simulations, thereby limiting its application for large-scale and 3D realistic models. Numerical Limit Analysis (NLA) is a specialized technique for analyzing collapse problems that offers an alternative to both LEM and FEM. It has demonstrated significant computational efficiency in resolving large-scale problems, while eliminating the necessity for assumptions concerning the failure mechanism, which makes it an appropriate tool for evaluating slope stability within a probabilistic methodology. Despite its advantages, few works have used NLA within probabilistic frameworks, with most of them focusing on the analysis of 2D slope stability problems (e.g. Huang et al., 2013; X. Wang et al., 2022). This study aims to explore the application of NLA within a probabilistic framework incorporating cross-correlated random fields and employing Monte Carlo Simulations (MCS) for 2D and 3D problems. The subsequent sections detailed some aspects of NLA, the generation of Random Fields and the adopted probabilistic framework. The implemented codes are validated in a 2D slope model and applied to analyze a large 3D slope.

## 2 NUMERICAL LIMIT ANALYSIS

The Numerical Limit Analysis is a method that employs plastic limit theorems and numerical techniques to estimate the collapse load. Static formulations of NLA establish a statically admissible stress field and kinematic formulations establish a kinematically compatible failure mechanism. Depending on the interpolation space chosen to discretize stresses and velocities, the collapse load obtained is a rigorous upper or lower bound of the actual collapse load. The NLA formulation employed in this study has been previously implemented in a MATLAB code (Araújo, 1997; Camargo et al., 2016; Carrión et al., 2017; Durand et al., 2006; Fernández et al., 2021, 2023; Gomes et al., 2017; Tapia et al., 2013). It discretizes the static theorem of limit analysis using a conventional finite element mesh and mixed interpolation for stresses ($\sigma$) and velocities ($\dot{u}$). The velocities are interpolated using linear interpolation functions, and stresses are considered constant for each element. Although this mixed-weak NLA formulation does not guarantee the estimation of a rigorous collapse load, it enables the derivation of approximate solutions and has demonstrated efficiency and precision in the analysis of stability problems in various types of geotechnical structures. The stability problem is formulated as a convex optimization problem:

$$\begin{aligned} &\text{maximize} && \lambda \\ &\text{subject to} && \boldsymbol{G}.\boldsymbol{\sigma} = \lambda\, \boldsymbol{f_f} + \boldsymbol{f_v} \\ & && F(\boldsymbol{\sigma}) \leq 0 \end{aligned} \qquad (1)$$

where $\lambda \in \mathbb{R}$ , represents the collapse factor applied to the loads inducing the structural collapse, $\boldsymbol{\sigma} \in \mathbb{R}^{\boldsymbol{n}}$ is the vector of stress components, $F(\boldsymbol{\sigma}) \in \mathbb{R}^{\boldsymbol{m}}$ is the function of failure criterion, $\boldsymbol{G} \in \mathbb{R}^{\boldsymbol{p}\times\boldsymbol{n}}$ is the equilibrium matrix, $\boldsymbol{f_v} \in \mathbb{R}^{\boldsymbol{p}}$ denotes a vector containing the structure's self-weight, $\boldsymbol{f_f} \in \mathbb{R}^{\boldsymbol{p}}$ is a fictitious nodal force vector magnified by the collapse factor, $m$ is the number of mesh elements, $n$ is the total number of stress components and $p$ is the total number of velocity components. The transformation of the convex optimization problem into a second-order cone programming (SOCP) can be achieved, as proposed by Makrodimopoulos & Martin (2006), by substituting the stress vector $\boldsymbol{\sigma} = \boldsymbol{D^{-1}\rho} - \boldsymbol{D^{-1}d}$, where $\boldsymbol{\rho}$ is an auxiliary vector, and arrays $\boldsymbol{D}$ and $\boldsymbol{d}$ facilitate the transformation of the rupture criterion. These arrays can be estimated from the Mohr-Coulomb parameters ($c$ , $\phi$). The resulting optimization problem is solved by the interior point conic optimization algorithm, implemented by Andersen et al. (2003). The collapse factor $\lambda$ is obtained directly from this optimization process, along with the velocities resulting from the dual optimization problem. The safety factor can also be obtained via strength reduction technique, as explained in Fernández et

al. (2023). The collapse mechanisms are identified by plotting the normalized velocities within the model geometry.

## 3 RANDOM FIELDS MODEL

The Random Field theory is a powerful tool for characterizing the spatial variability of soil material (Vanmarcke, 1984). A random field $\boldsymbol{X}$ is a mathematical model that assigns random values to each point or location within a specified domain or spatial extent. To define a RF, overall statistics such as the mean ($\mu$), the standard deviation (σ), or the coefficient of variation (COV), and the scale of fluctuation SOF (δ) are considered. The SOF provides insight into the range over which prominent fluctuations or changes in parameters occurs. This study employs the Covariance Decomposition Method to create RFs, and it involves the following components: (**1) Definition of the Autocorrelation Matrix (C)**, which is the representation of the spatial correlation structure in a RF. It provides information about the degree of similarity between the RF values at different locations, considering only the distance between them, and is defined through autocorrelation functions (ACFs) as the single exponential (Eq.2) and Second-order Markov (Eq.3), lags Δx, Δy and Δz are the distances between two locations, while δx, δy and δz are the SOF, in the x, y and z directions, respectively.

$$\rho(\Delta x, \Delta y, \Delta_z) = \exp\left[-2\left(\frac{\Delta x}{\delta x} + \frac{\Delta y}{\delta y} + \frac{\Delta z}{\delta z}\right)\right] \tag{2}$$

$$\rho(\Delta x, \Delta y, \Delta z) = \exp\left[-4\left(\frac{\Delta x}{\delta x} + \frac{\Delta y}{\delta y} + \frac{\Delta z}{\delta z}\right)\right]\left(1 + \frac{4\,\Delta x}{\delta x}\right)\left(1 + \frac{4\,\Delta y}{\delta y}\right)\left(1 + \frac{4\,\Delta z}{\delta z}\right) \tag{3}$$

The autocorrelation coefficient is evaluated at each location and the resulting matrix C has dimensions $n_e \times n_e$, where $n_e$ represents the total number of points at which the random field is discretized. In the conventional CMD the discretization process employed follows a midpoint approach, where each realization of **X** is represented as a piecewise constant and defined at the centroid of each element. **(2) Definition of the Cross-correlation Matrix (R)**, it is possible to include cross-correlation between different parameters at the same location through the definition of the Cross-correlation matrix. This matrix, containing the correlation coefficients, has dimensions $n_p \times n_p$, where $n_p$ represents the total number of correlated parameters**. (3) Cholesky decomposition and cross-correlated Random Fields generation**, Cholesky decomposition algorithm is used to factorize the matrices $\boldsymbol{C = L_1\, L_1^T}$ and $\boldsymbol{R = L_2\, L_2^T}$**,** in order to obtain the lower triangular matrices $\mathbf{L_1}$ and $\mathbf{L_2}$, with $n_e \times n_e$ and $n_p \times n_p$ dimensions, respectively. A cross-correlated gaussian, multivariate RF is obtained as $\boldsymbol{X = L_1\, \xi\, L_2^T}$, where $\boldsymbol{\xi}$ is a matrix of standard normal random samples, with a dimension of $n_e \times n_p$. The RF obtained can be transformed into a Lognormal (Non-Gaussian) RF, through isoprobabilistic transformation. The simulation of large-scale and high-resolution RFs by the conventional CMD method demands substantial computational resources, alternatively the **Stepwise Covariance Matrix Decomposition method** offers an innovative approach, as explained in detail in Li et al. (2019) .

## 4 PROBABILISTIC FRAMEWORK

The probabilistic framework proposed encompasses three primary components: random fields generation, stability evaluation utilizing NLA, and failure function assessment. Whitin the RFs generation component, marginal distribution of random variables, SOF values, and cross-correlation coefficients are defined. Additionally, the selection of the CMD method to be employed is also made. If conventional CMD is chosen, the definition of the RFs is directly performed at the centroid of each finite element of the mesh, which will subsequently be utilized in the stability analysis. If stepwise CMD is selected, an auxiliary lattice mesh is created, and once the RFs values within it are defined, they are mapped to the centroid of the finite element mesh used for the stability analysis. In the stability evaluation component, additional deterministic parameters and boundary conditions are included. Collapse mechanisms, collapse factors, and safety factors are then obtained for each simulation. Finally, using the results from previous NLA simulations and the defined failure function, the probability of failure is estimated. The failure function may be defined based on the estimation of the safety factor as $Fs - 1 = 0$. Alternatively, it is possible to determine the failure function in terms of the collapse factor as $\lambda = 0$.

## 5 VALIDATION AND APLICATION EXAMPLES

This section is dedicated to the validation and application of the proposed probabilistic framework and the implemented codes. Initially, validation was conducted through probabilistic slope stability analysis on a 2D slope problem. Subsequently, a large 3D slope was analyzed. The simulations were executed in an Intel-i9-12900-CPU@2.40 GHz processor.

### 5.1 Analysis of a 2D slope

In order to validate the implemented codes, a 2D slope problem, previously studied by Cho (2010) with Random Limit Equilibrium Method (RLEM), was examined. Figure 1 (a) depicts the geometry and the finite element mesh utilized for the analysis, consisting of 7,826 bilinear quadrilateral elements and 8,038 nodes, with an average finite element size of 0.20 m. The sides at $x = 0$ m, $x = 30$ m, and $y = 0$ m, have restricted velocities in the x and y directions. In this example, cohesion and friction angle were represented through cross-correlated RFs, with a mean cohesion $\mu_c = 10$ kPa and a coefficient of variation $COV_c = 0.3$, a mean friction angle $\mu_\phi = 30°$ with a coefficient of variation $COV_c = 0.2$ and a cross-correlation coefficient between cohesion and friction angle $\rho_{c\phi} = -0.5$. The unit weight was assumed as a deterministic value of $\gamma = 20\ kN/m^3$. For the generation of RFs a single exponential function was implemented, with $\delta_x = 40$ m and $\delta_y = 4$ m, horizontal and vertical SOF, respectively. 5,000 MCS were conducted and the results obtained are presented in Table 1.

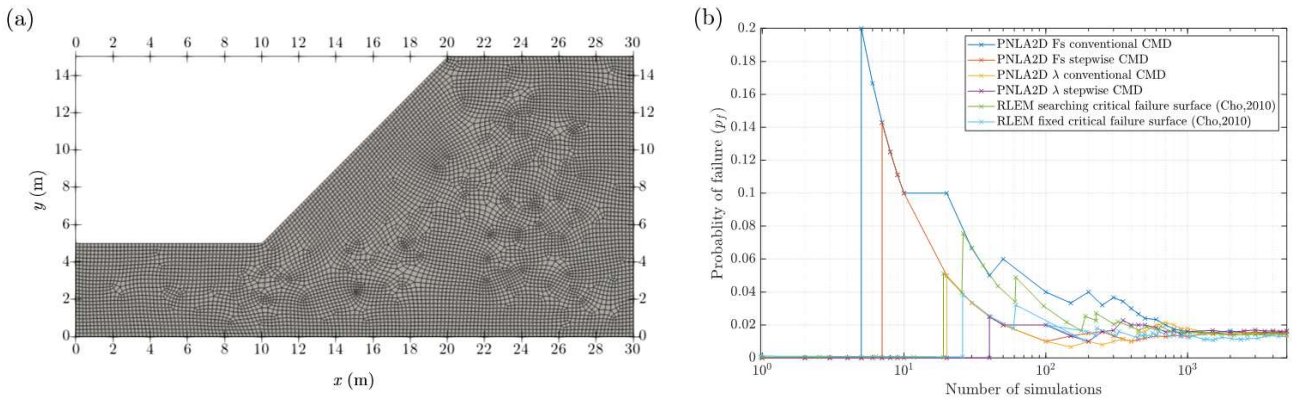


Figure 1. (a) Geometric configuration and finite element mesh utilized in the 2D probabilistic slope stability analysis (b) Convergence plots of probability of failure (pf).

As a result of PNLA-2D, the probability of failure was calculated through MCS, considering a failure function based on the safety factor and the collapse factor estimations, using both conventional and stepwise CMD. For conventional CMD the RFs were discretized at the centroid of each finite element, in this case, maintaining a relationship between finite element size and scale of fluctuation small enough to minimize the variance reduction effect due to local averaging within the element. For stepwise CMD an auxiliar grid mesh was created with an element size of 0.20 meters. The mean safety factor (Fs mean) and its standard deviation (Fs std), as estimated by Cho (2010) using the Random Limit Equilibrium Method (RLEM) with both a searching the critical failure surface and fixing the critical surface approaches, exhibit a noteworthy consistency with those estimated by the PNLA-2D code. Regarding the probability of failure, the results derived from PNLA-2D lie within the pf values obtained by RLEM. The probability of failure values obtained by stepwise CMD were higher than those estimated by conventional CMD. Analysis with PNLA-2D considering a failure function based on the collapse factor and generating RFs with the stepwise CMD method, provided a reasonable estimation of the probability of failure in a shorter time, 5,000 MCS were conducted within a period of fewer than one hour. Figure 1 (b) depicts the convergence plots of the probability of failure for the implemented methodologies and the RLEM results. Figure 2 shows two typical simulation results with PNLA-

2D, including the cohesion and friction angle RFs and their respective rupture surface. Irregular-shaped failure surfaces were identified, which differ from the usual circular shapes assumed in RLEM.

Table 1. Summary of simulation results for the 2D model

| | Analysis | Number of simulations | pf | Fs/$\lambda$ mean | Fs/$\lambda$ std | t (hours) |
|---|---|---|---|---|---|---|
| Cho (2010) | RLEM (searching the critical failure surface) | 50,000 | 0.017 | 1.20 | 0.10 | - |
| Cho (2010) | RLEM (performed for the fixed critical surface) | 50,000 | 0.014 | 1.21 | 0.11 | - |
| PNLA - 2D | Fs conventional CMD | 5,000 | 0.014 | 1.19 | 0.10 | 8.12 |
| PNLA - 2D | Fs stepwise CMD | 5,000 | 0.016 | 1.19 | 0.10 | 6.01 |
| PNLA - 2D | $\lambda$ conventional CMD | 5,000 | 0.014 | 1.86 | 0.76 | 3.82 |
| PNLA - 2D | $\lambda$ stepwise CMD | 5,000 | 0.016 | 1.87 | 0.81 | 0.92 |

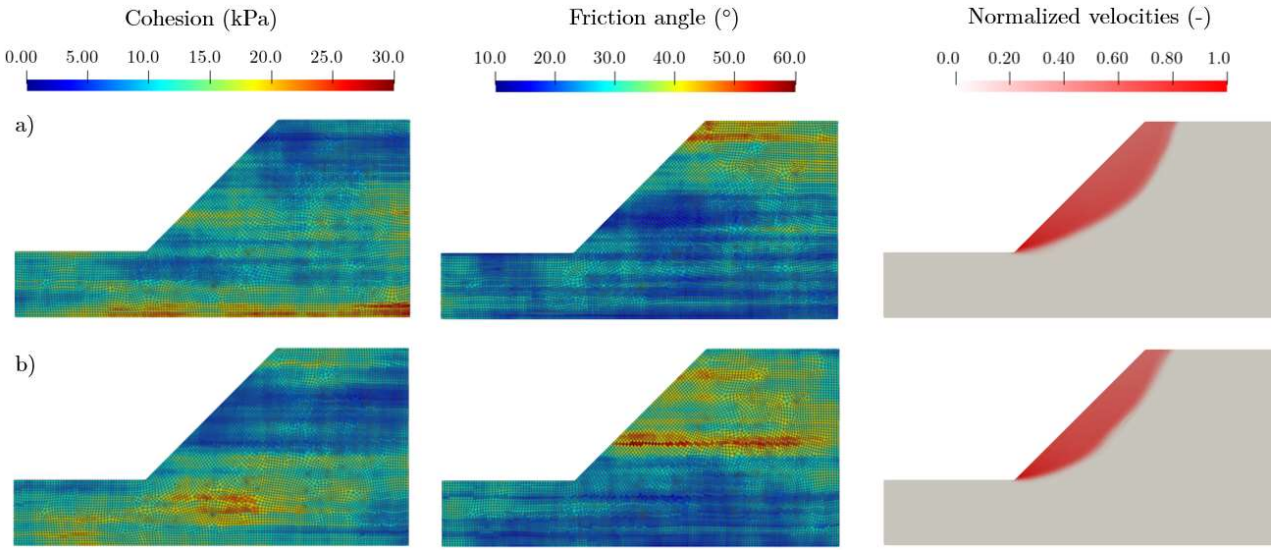


Figure 2. Typical realizations of cross-correlated bivariate RFs and their rupture mechanisms obtained with the PNLA-2D code. (a) Fs = 1.02, conventional CMD (b) Fs=1.27 stepwise CMD.

### 5.2 Analysis of a large 3D slope

In this section, the stability of a large 3D slope is examined, utilizing a model based on previous studies by Hicks & Spencer (2010) and Varkey et al (2018). The analysis was conducted using the PNLA-3D code, with RFs generated through the stepwise CMD method. Figure 3 (a) illustrates the model geometry and the finite element mesh utilized, comprising 7,550 brick elements and 9,129 nodes. The RFs were generated using an auxiliary mesh of 0.50 m. The sides at $x = 10$ m, $y = 0$ m, $y = 50$ m, and $z = 0$ m have restricted velocities in the x, y, and z directions. The cohesion and friction angle were represented through cross-correlated RFs, considering a mean cohesion $\mu_c = 5$ kPa and a coefficient of variation $COV_c = 0.2$, a mean friction angle $\mu_\phi = 30°$ and a coefficient of variation $COV_\phi = 0.2$. The unit weight was assumed as a deterministic value of $\gamma = 20\ kN/m^3$. A second-order Markov autocorrelation function was employed to generate RFs. To assess the influence of various horizontal SOF, the degree of anisotropy of the heterogeneity value ($\xi$) was introduced, representing the ratio between the horizontal ($\delta_x = \delta_y = \delta_h$) and vertical ($\delta_z = \delta_v$) SOF. The vertical SOF was fixed at $\delta_v = 2$ m, while horizontal SOF of 2 m, 20 m and 100 m were evaluated, corresponding to $\xi =$

1, $\xi = 10$ , and $\xi = 50$, respectively. Three values of the cross-correlation coefficient were considered in the analysis: $\rho_{c\phi} = -0.5$, $\rho_{c\phi} = 0$ and $\rho_{c\phi} = 0.5$.

Sets of 1,000 simulations were conducted for each combination of $\xi$ and $\rho_{c\phi}$, each simulation lasted about 17 seconds. The probability density function of the safety factor obtained for each case is presented in Figure 3 (b-d). For cases where a positive value of $\rho_{c\phi}$ was considered, distributions with lower mean safety factor values, and higher probability of failure were obtained. Conversely, when a negative value of $\rho_{c\phi}$ was implemented, the opposite effect was observed. The magnitude of $\xi$, and therefore the magnitude of the horizontal scale of fluctuation, significantly influences the dispersion of the safety factor distribution. The coefficient of variation estimated for the safety factor distributions varies from 1.5% to 8% when considering $\xi = 1$ and $\xi = 50$, respectively, while maintaining $\rho_{c\phi} = -0.5$. Figure 4 shows two typical results obtained with PNLA-3D. These results include the cohesion and friction angle RFs alongside their respective failure surfaces. Discrete failure surfaces were identified at various zones of the slope, and their positions were directly correlated with the spatial distribution of the parameters obtained during the generation of RFs. The maximum probability of failure, estimated considering $\xi = 50$ and $\rho_{c\phi} = 0.5$, was 3.9%.

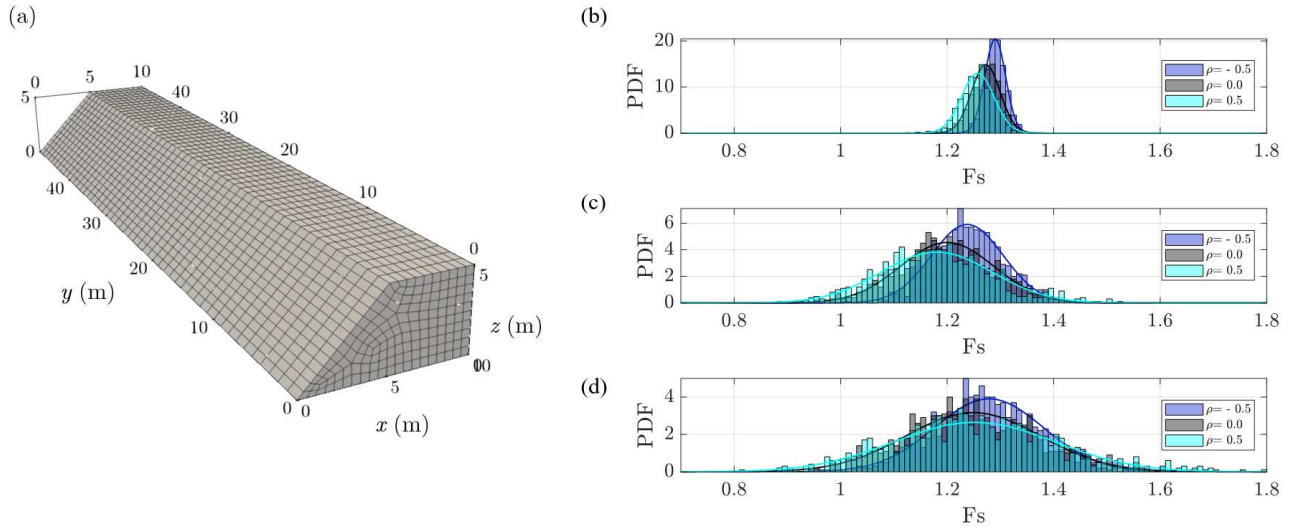


Figure 3. Geometric configuration and results obtained in the 3D probabilistic slope stability analysis. (a) Finite element mesh utilized, composed by 7550 brick elements and 9129 nodes. Safety factor probability density functions obtained for each case, considering different degrees of anisotropy of the heterogeneity: (b) $\xi = 1$, (c) $\xi = 10$ and (d) $\xi = 50$.

## 6 DISCUSSION AND CONCLUSIONS

In this study, a probabilistic numerical limit analysis PNLA code has been developed for analyzing 2D and 3D slope stability problems, considering the spatial variability of soil shear strength parameters. The probabilistic framework proposed, integrates the covariance matrix decomposition (CMD) method, along with the numerical limit analysis (NLA) and Monte Carlo Simulations (MCS), to evaluate the probability of failure and the safety factor distribution. The PNLA code was initially validated using a 2D slope stability model. The safety factor statistics and estimations of the probability of failure made with PNLA closely approximated those presented by Cho (2010), who used the Random Limit Equilibrium Method (RLEM). However, PNLA simulations provide more realistic definitions of rupture mechanisms, as RLEM cannot identify irregular rupture surfaces. This aspect could have significant implications in consequence analysis within a risk evaluation framework. The application example of the 3D large slope presented allows for the verification of the significant influence of the scale of fluctuation and the cross-correlation coefficient magnitudes. Adopting a positive cross-correlation coefficient between shear strength parameters increases the estimated probability of failure. Meanwhile, a higher degree of anisotropy of the heterogeneity values, and therefore a higher horizontal scale of fluctuation values, significantly affects the dispersion of the safety factor distribution.

Within the analysis methodologies presented in this study, integrating stepwise CMD with a failure function based on the collapse factor emerges as an efficient approach for assessing the probability of failure in large-scale, high-resolution problems.

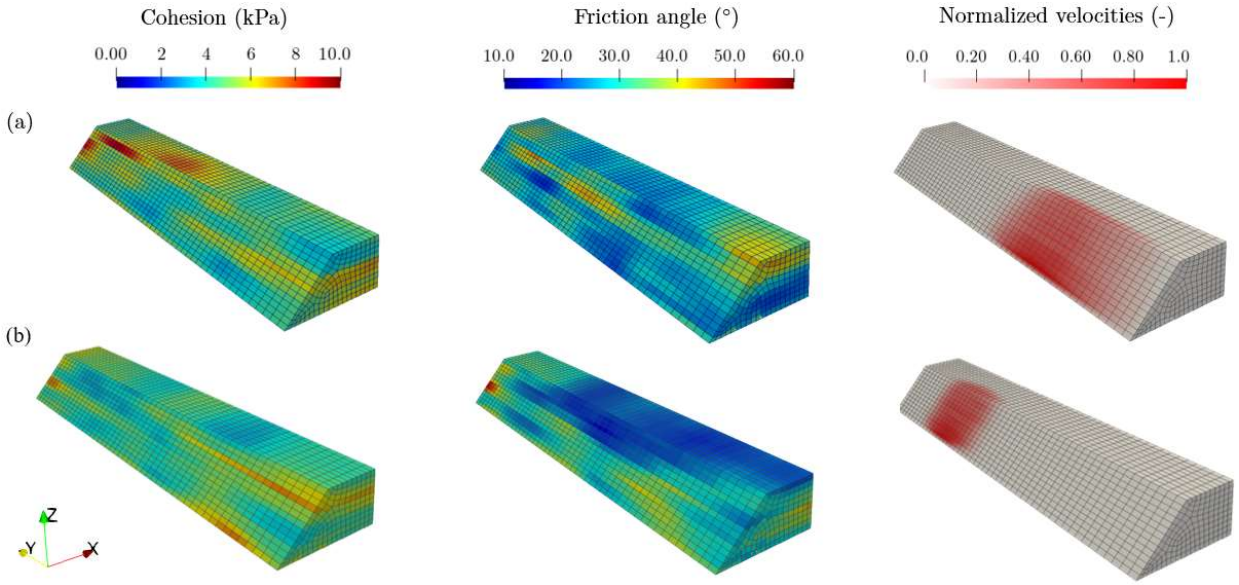


Figure 4. Typical realizations of cross-correlated bivariate RFs and its rupture mechanisms obtained in the PNLA-3D code. (a) $\xi = 10,\ \rho_{c\phi} = -0.5,\ \mathrm{Fs} = 1.17$, (b) $\xi = 10,\ \rho_{c\phi} = 0.5,\ \mathrm{Fs} = 1.11$.

**Acknowledgments:** This study was financed in part by the Coordenação de Aperfeiçoamento de Pessoal de Nível Superior - Brasil (CAPES) - Finance Code 001.

## REFERENCES

Andersen, E. D., Roos, C., & Terlaky, T. (2003). On implementing a primal-dual interior-point method for conic quadratic optimization. *Mathematical Programming*, *95*, 249–277.

Araújo, L. G. (1997). *Numerical study of stability problems in rock mass using limit analysis*. PhD Thesis. Department of Civil Engineering, Pontifícia Universidade Católica do Rio de Janeiro.

Camargo, J., Velloso, R. Q., & Vargas, E. A. (2016). Numerical limit analysis of three-dimensional slope stability problems in catchment areas. *Acta Geotechnica*, *11*, 1369–1383.

Carrión, M., Vargas, E. A., Velloso, R. Q., & Farfán, A. D. (2017). Slope stability analysis in 3D using numerical limit analysis (NLA) and Elastoplastic analysis (EPA). *Geomechanics and Geoengineering*, *12*(4), 250–265.

Cho, S. E. (2007). Effects of spatial variability of soil properties on slope stability. *Engineering Geology*, *92*(3), 97–109. https://doi.org/https://doi.org/10.1016/j.enggeo.2007.03.006

Cho, S. E. (2010). Probabilistic assessment of slope stability that considers the spatial variability of soil properties. *Journal of Geotechnical and Geoenvironmental Engineering*, *136*(7), 975–984.

Durand, A. F., Vargas Jr, E. A., & Vaz, L. E. (2006). Applications of numerical limit analysis (NLA) to stability problems of rock and soil masses. *International Journal of Rock Mechanics and Mining Sciences*, *43*(3), 408–425.

El-Ramly, H., Morgenstern, N. R., & Cruden, D. M. (2002). Probabilistic slope stability analysis for practice. *Canadian Geotechnical Journal*, *39*(3), 665–683. https://doi.org/10.1139/t02-034

Fernández, F., Calpa, D. S., Vargas Jr, E., Velloso, R. Q., & Dias, D. (2023). Basal Heave Stability Analysis of a Circular Shaft Excavation Considering FEM, NLA, and MPM Approaches. *Geotechnical and Geological Engineering*, 1–22.

Fernández, F., Rojas, J. E. G., Vargas, E. A., Velloso, R. Q., & Dias, D. (2021). Three-dimensional face stability analysis of shallow tunnels using numerical limit analysis and material point method. *Tunnelling*

*and Underground Space Technology*, *112*, 103904. https://doi.org/https://doi.org/10.1016/j.tust.2021.103904

Gomes, G. J. C., Vrugt, J. A., Vargas, E. A., Camargo, J. T., Velloso, R. Q., & van Genuchten, M. Th. (2017). The role of uncertainty in bedrock depth and hydraulic properties on the stability of a variably-saturated slope. *Computers and Geotechnics*, *88*, 222–241. https://doi.org/https://doi.org/10.1016/j.compgeo.2017.03.016

Griffiths, D. V, & Fenton, G. A. (2000b). Influence of soil strength spatial variability on the stability of an undrained clay slope by finite elements. In *Slope stability 2000* (pp. 184–193).

Griffiths, D. V, & Fenton, G. A. (2004). Probabilistic slope stability analysis by finite elements. *Journal of Geotechnical and Geoenvironmental Engineering*, *130*(5), 507–518.

Hicks, M. A., & Samy, K. (2002). Influence of heterogeneity on undrained clay slope stability. *Quarterly Journal of Engineering Geology and Hydrogeology*, *35*(1), 41–49.

Hicks, M. A., & Spencer, W. A. (2010). Influence of heterogeneity on the reliability and failure of a long 3D slope. *Computers and Geotechnics*, *37*(7–8), 948–955.

Huang, J., Lyamin, A. V, Griffiths, D. V, Krabbenhoft, K., & Sloan, S. W. (2013). Quantitative risk assessment of landslide by limit analysis and random fields. *Computers and Geotechnics*, *53*, 60–67.

Jiang, S.-H., & Huang, J. (2018). Modeling of non-stationary random field of undrained shear strength of soil for slope reliability analysis. *Soils and Foundations*, *58*(1), 185–198.

Li, D.-Q., Jiang, S.-H., Cao, Z.-J., Zhou, W., Zhou, C.-B., & Zhang, L.-M. (2015). A multiple response-surface method for slope reliability analysis considering spatial variability of soil properties. *Engineering Geology*, *187*, 60–72.

Li, D.-Q., Xiao, T., Zhang, L.-M., & Cao, Z.-J. (2019). Stepwise covariance matrix decomposition for efficient simulation of multivariate large-scale three-dimensional random fields. *Applied Mathematical Modelling*, *68*, 169–181.

Makrodimopoulos, A., & Martin, C. (2006). Lower bound limit analysis of cohesive-frictional materials using second-order cone programming. *International Journal for Numerical Methods in Engineering*, *66*(4), 604–634.

Ou-Yang, J.-Y., Liu, Y., Yao, K., Yang, C.-J., & Niu, H.-F. (2021). Model Updating of Slope Stability Analysis Using 3D Conditional Random Fields. *ASCE-ASME Journal of Risk and Uncertainty in Engineering Systems, Part A: Civil Engineering*, *7*(3), 4021034.

Tang, X.-S., Wang, M.-X., & Li, D.-Q. (2020). Modeling multivariate cross-correlated geotechnical random fields using vine copulas for slope reliability analysis. *Computers and Geotechnics*, *127*, 103784.

Tapia, M., Júnior, E. do A. V., & Vaz, L. E. (2013). *Análise de confiabilidade de taludes em condições saturadas-não saturadas via análise limite no espaço cônico quadrático*. PUC-Rio.

Vanmarcke, E. H. (1984). Random Fields: New Concepts and Engineering Applications. *Probabilistic Mechanics and Structural Reliability*, 7–17.

Varkey, D., Hicks, M. A., & Vardon, P. J. (2018). 3D slope stability analysis with spatially variable and cross-correlated shear strength parameters. In *Numerical Methods in Geotechnical Engineering IX, Volume 1* (pp. 543–549). CRC Press.

Wang, M. Y., Liu, Y., Ding, Y. N., & Yi, B. L. (2020). Probabilistic stability analyses of multi-stage soil slopes by bivariate random fields and finite element methods. *Computers and Geotechnics*, *122*. https://doi.org/10.1016/j.compgeo.2020.103529

Wang, X., Xia, X., Zhang, X., Gu, X., & Zhang, Q. (2022). Probabilistic Risk Assessment of Soil Slope Stability Subjected to Water Drawdown by Finite Element Limit Analysis. *Applied Sciences*, *12*(20), 10282.

Wang, Z.-Z., & Goh, S. H. (2021). Novel approach to efficient slope reliability analysis in spatially variable soils. *Engineering Geology*, *281*, 105989. https://doi.org/https://doi.org/10.1016/j.enggeo.2020.105989

Zhu, D., Xia, L., Griffiths, D. V, & Fenton, G. A. (2021). Reliability analysis of infinite slopes with linearly increasing mean undrained strength. *Computers and Geotechnics*, *140*, 104442. https://doi.org/https://doi.org/10.1016/j.compgeo.2021.104442.